Indian J. pure appl. Math., 23(6): 443-462, June 1992

TRANSITIONS IN HEAT TRANSFER IN A ROTATING POROUS LAYER

P. K. Srimani and H. R. Sudhakar

Department of Mathematics, UGC-DSA, Centre in Fluid Mechanics
Central College, Bangalore University, Bangalore 560 001

(*Received* 4 *February* 1991; *accepted* 2 *December* 1991)

Transitions in heat transfer in a rotating horizontal porous layer is investigated analytically using the modified Galerkin Technique. Critical conditions for the onset of steady and oscillatory convection are determined and it is found that subcritical motions are not possible in physical situations; a rotating porous layer also suffers transitions in heat transfer similar to the viscous layer, and the non-linear momentum advection term has negligible effect on the results.

1. Introduction

In the present day power crisis, attention is drawn towards innovational and economically feasible methods of generating power. Broadly speaking, all the heat that is trapped in the earth's interior can be regared as geothermal resources. The problem associated with such phenomena is convective instability.

Convection in a porous layer has a very wide range of applications (see Rudraiah and Srimani[7], Srimani[10]). The Coriolis force caused by earth's rotation significantly alters the quantitative nature of heat transfer. Therefore, a realistic geothermal model should include these effects. In an ordinary viscous flow, the effect of rotation is fully explored (see Chandrasekhar[3] and Turner[11]) but attention is not focussed to study its effect on convection in a porous medium and observations in this regard are lacking. The first linear stability analysis in the case of thermal convection in a rotating fluid saturated porous medium was performed by Rudraiah and Srimani[7]. They have investigated the effect of Coriolis force on the onset of convection by employing the standard technique of normal mode expansion. It is well known that linear stability theory can yield useful information on the critical parameters and convective patterns at the onset of cellular convection. Therefore a thorough investigation of the fully nonlinear problem is essential and this is investigated in this paper. It is well known that instability sets in only when the Rayleigh number exceeds its critical value and when the flow is established, the fluid exhibits a striking array of convection cells which are spatially periodic. As long as there is no external constraint such as rotation or magnetic field or salinity gradient acting on the system to offset the destabilizing nature of potential energy, the pattern of convection remains uniform i.e., the cell boundaries will not be distorted and the principle of exchange of stability is said to be valid. In that case, there will be a complete balance between the

potential energy released and the Darcy resistance; temperature and velocity fields will be in phase.

Thus the foregoing discussion reveals that convection mechanisms in the non-rotating and rotating systems are entirely different and therefore one has to investigate these two aspects separately. Since the aim of our study is for a clear apprehension of convection in geothermal regions, the transitions in heat transfer, the effect of Coriolis force on the nonlinear thermal convection in a porous medium is investigated in detail in this paper. (Rudraiah and Srimani[7] hereafter called I).

The method employed is the modified power integral technique which also combines the best features of Galerkin technique. The unique feature of this method is that excellent agreement with the experimental results could be achieved for a very wide range of the parameters analytically. So far, no work is available in this direction.

Section 2 deals with the mathematical formulation. Section 3, deals with the linear stability analysis. Section 4, deals with the general finite amplitude solution. Section 5, deals with finite amplitude solution for rolls. Section 6, deals with the heat transport. In Section 7, a detailed discussion of the results is presented.

2. Mathematical Formulation

The physical configuration is shown schematically in Fig. 1. Under the assumptions and approximations cited in I, the governing dimensionless equations

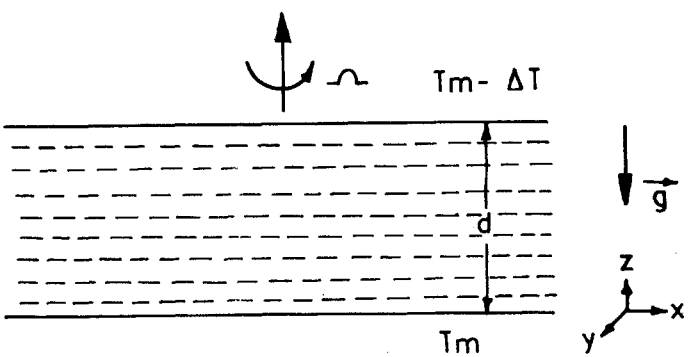

Fig. 1. Geometry of fluid motion

of the problem of discrete transitions in the heat transfer in a fluid saturated porous layer rotating with an uniform angular velocity $\vec{\Omega}$ about the vertical z-axis and subject to an adverse temperature gradient are :

$$(\partial/\partial t - \nabla^2)\, T - \sigma\lambda^* W = \sigma^2\, [\{WT\}_m - \overline{WT}] - \sigma h \qquad \ldots(2.1)$$

$$(\sigma^{-1}\, \partial/\partial t + 1/P_L)\, \nabla^2 W + \mathcal{J}\, \frac{\partial W}{\partial z} = -\sigma^{-1}\, \nabla_1^2\, T = L \qquad \ldots(2.2)$$

$$(\sigma^{-1}\, \partial/\partial t + 1/P_L)\, \zeta - \mathcal{J}\, \frac{\partial W}{\partial z} = -Z \qquad \ldots(2.3)$$

$$\nabla \cdot \vec{q} = 0 \qquad \ldots(2.4)$$

where $$h = \vec{q} \cdot \vec{\nabla} T - \frac{\partial}{\partial z}\, (\overline{WT})$$

represents the zero-average heat advection term,

$$L = \frac{\partial}{\partial z}\left[\frac{\partial}{\partial x}(\vec{q}\cdot\nabla u) + \frac{\partial}{\partial y}(\vec{q}\cdot\nabla u)\right] - \nabla_1^2(\vec{q}\cdot\nabla W)$$

represents the zero-average momentum advection term,

$$Z = \frac{\partial}{\partial x}(\vec{q}\cdot\nabla v) - \frac{\partial}{\partial y}(\vec{q}\cdot\nabla u)$$

is a zero average non linear term;

d = depth of the porous layers;

$$E = -\left[\frac{1}{P_L^2}(9\alpha^2 + 1)^2 + y^2(9\alpha^2 + 1) - \frac{9\alpha^2\lambda_0^*}{\pi^2 p_L}\right]$$

$\vec{q}$ = mean filter velocity of the fluid, (u, v, W);

t = time;

k = permeability of the porous medium;

κ = the effective thermal conductivity of a fluid in the presence of a porous medium which is the sum of the stagnant thermal conductivity due to molecular diffusion and thermal dispersion coefficient due to mechanical dispersion;

$T = T(z) + T(x, y, z, t)$ is the deviation of the temperature from its mean value;

α = the thermal expansion coefficient;

β = the adverse temperature gradient;

ν = the kinematic viscosity of the fluid;

ρ = the density;

ρ_m = the mean density;

$(\rho c)_f$ = heat capacity of the fluid;

$\vec{\Omega}$ = uniform angular velocity of the system, $(0, 0, \Omega)$;

$\zeta = \frac{\partial v}{\partial x} - \frac{\partial u}{\partial y}$, the vertical component of vorticity;

$\lambda^* = \alpha g\beta(\rho c)_f d^2k/\nu k$, the Rayleigh number;

$1/P_L = d^2/k$, the porous parameter;

∇^2 = the three-dimensional Laplacian Operator;

$$\partial^2/\partial x^2 + \partial^2/\partial y^2 + \partial^2/\partial z^2;$$

$\nabla_1^2 = \partial^2/\partial x^2 + \partial^2/\partial y^2$; $\rho = \rho_m(1 - \alpha\tilde{T})$;

is the equation of state and

$$E_m = \frac{1}{8\pi lm}\int_{-l}^{l}\int_{-m}^{m}\int_{0}^{2\pi}(\;)\,dx\,dy\,dt$$

is the ensemble average which denotes an average over the horizontal space and time periods; l and m are the horizontal and vertical components of the horizontal wave number α.

In this process $T(z)$ denotes the ensemble average temperature and $\overline{T(x,y,z,t)} = 0$; where the overbar denotes an ensemble average and $(\ )_m$ denotes both an enselble and vertical average.

As we are interested in the local nonlinear stability analysis, it is convenient to consider the equation for the vertical component of velocity obtained by eliminating T in the above set of equations.

That is,

$$(\sigma^{-1}\,\partial/\partial t + 1/P_L)^2\,(\partial/\partial t - \nabla^2)\,\nabla^2 W + \mathcal{J}^2\,(\partial/\partial t - \nabla^2)\,\frac{\partial^2 W}{\partial z^2}$$

$$- (\sigma^{-1}\,\partial/\partial t + 1/P_L)\,\nabla_1^2\,W = (\sigma^{-1}\,\partial/\partial t + 1/P_L)\,[\{WT\}_m - \overline{WT}]\nabla_1^2 W$$

$$+ (\partial/\partial t - \nabla^2)\,\frac{\partial Z}{\partial z} - (\sigma^{-1}\,\partial/\partial t + 1/P_L)\,\nabla_1^2\,h$$

$$+ (\partial/\partial t - \nabla^2)\,(\sigma^{-1}\partial/\partial t + 1/P_L)L. \qquad \ldots(2.5)$$

We seek the solutions in the form

$$\left.\begin{aligned} f &= \epsilon f_0 + \epsilon^2 f_1 + \epsilon^3 f_2 + \ldots \\ \lambda^* &= \lambda_0^* + \epsilon\lambda_1^* + \epsilon^2\lambda_2^* + \ldots \end{aligned}\right\} \qquad \ldots(2.6)$$

where ϵ is a constant parameter identified with the amplitude and is to be determined by the values of λ^* and λ_i^*.

Boundary Conditions :

The boundaries are assumed to be stress-free. perfectly conducting boundaries and hence

$$\left.\begin{aligned} W &= 0, \text{ at } z = 0,\ 1; \\ T &= 0 \text{ at } z = 0,\ 1. \end{aligned}\right\} \qquad \ldots(2.7)$$

3. Linear Stability Analysis

In this section, we solve the linear stability problem, the solutions of which are of great importance in the finite amplitude study, by using the local nonlinear stability analysis.

Substituting (2.6) into (2.1) to (2.4) and equating the like powers of ϵ, we arrive at a set of equations corresponding to different orders of ϵ.

The linear equations obtained by considering only the first-order terms in ϵ are

$$(\partial/\partial t - \nabla^2)\,T_0 - T\lambda_0^*\,W_0 = 0. \qquad \ldots(3.1)$$

$$(\sigma^{-1}\,\partial/\partial t + 1/P_L)\,\zeta_0 - \mathcal{J}\,\frac{\partial W_0}{\partial z} = 0 \qquad \ldots(3.2)$$

$$(\sigma^{-1}\partial/\partial t + 1/P_L)^2 (\partial/\partial t - \nabla^2) \nabla^2 W_0 + \mathcal{J}^2 (\partial/\partial t - \nabla^2) \frac{\partial^2 W_0}{\partial z^2}$$

$$- (\sigma^{-1} \partial/\partial t + 1/P_L) \lambda_0^* \nabla_1^2 W_0 = 0 \qquad \ldots(3.3)$$

$$\frac{\partial u_0}{\partial x_0} + \frac{\partial u_0}{\partial y_0} + \frac{\partial W_0}{\partial z_0} = 0. \qquad \ldots(3.4)$$

The assumption made in solving the stability problem is, the separability of horizontal and vertical dependence and periodicity in horizontal structure. Therefore, we write

$$W_0 = e^{p_0 t} f(x, y) g(z) \qquad \ldots(3.5)$$

where f satisfies the membrane equation,

$$\nabla_1^2 f(x, y) = - \alpha^2 \pi^2 f(x, y) \qquad \ldots(3.6)$$

where the separation parameter α is the effective wave number of the disturbance in the horizontal plane, p_0 is the frequency of oscillations and $f(x, y)$ is treated as a normalized function. By taking $g(z) = \sin n\pi z$ in (3.5), the free boundary conditions on w_0 will be satisfied and the substitution of this into (3.3) yields after some rearrangement, the following cubic equation p_0 :

$$p_0^3 + p_0^2 \left\{ \pi^3 (\alpha^2 + n^2) + \frac{2\sigma}{P_L} \right\}$$

$$+ P_0 \left\{ \frac{\sigma}{P_L} \left(\frac{\sigma}{P_L} + 2\pi^2 (\alpha^2 + n^2) \right) \right.$$

$$\left. + \frac{\sigma}{(\alpha^2 + n^2)} (\mathcal{J}^2 n^2 \sigma - \alpha^2 \lambda_0^*) \right\}$$

$$+ \left\{ \pi^2 \sigma^2 (\alpha^2 + n^2)/P_L + \pi^2 \sigma^2 y^2 n^2 - \frac{\alpha^2 \sigma^2 \lambda_0^*}{P_L (\alpha^2 + n^2)} \right\}. \qquad \ldots(3.7)$$

The solution of (3.7) decides the condition for the occurence of steady or overstable motions.

Steady Convective Instability

The condition for the onset of convection is obtained from (3.7) by setting $p_0 = 0$, i.e.,

$$\frac{\lambda_0^*}{\pi^4} = \frac{(\alpha^2 + n^2)}{\alpha^2 P_L} \left[(\alpha^2 + n^2) + \mathcal{J}_1^2 P_{L_1}^2 n^2 \right] \qquad \ldots(3.8)$$

where $\mathcal{J}_1^2 = \mathcal{J}^2/\pi^4$ and $P_{L_1} = \pi^2 P_L$.

The value of

$$\alpha^2 (\mathcal{J}^2, n^2, P_{L_1})$$

which minimizes λ_0^*/π^4 is obtained from

$$\frac{\partial \lambda_0^*}{\partial \alpha^2} = \frac{\alpha^4 - n^4}{P_{L_1}} - \mathcal{J}_1^2 \, n^4 \, P_{L_1} = 0 \qquad \ldots(3.9)$$

and α is given by

$$\alpha^2 = n^2 \, (1 + \mathcal{J}_1^2 \, P_{L_1}^2)^{1/2}.$$

From (3.8) and (3.10), the asymptotic expressions for α^2 and λ_0^* are given by

$$\alpha^2 \to \mathcal{J} P_L \, n^2, \; \lambda_0^*/\pi^4 \to \mathcal{J}_1^2 \, n^2 \, P_{L_1} \text{ as } \mathcal{J} \to \infty.$$

From the above relation we can conclude as in the case of viscous fluid (Veronis[12]) that the increase in the Taylor number causes a decrease in the cellular diameter. Also, both α^2 and λ_0^* are of higher order in $\mathcal{J}$, in the asymptotic range. The curves in Fig. 2, show the dependence of λ_0^*/π^4 on $\mathcal{J}_1^2$, for a number of values of the porous

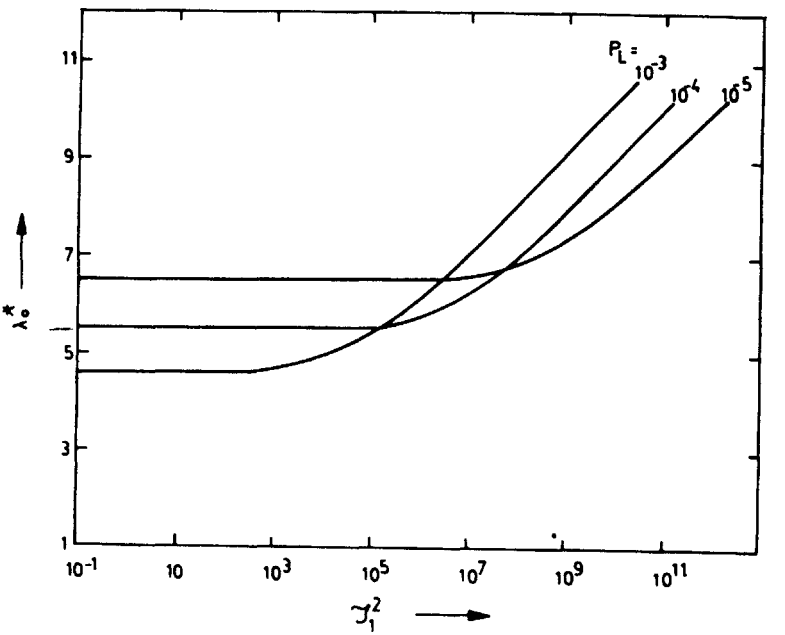

FIG. 2. λ_0 vs $\mathcal{J}_1^2$ for the steady case.

parameter P_L when $n=1$ which corresponds to the most unstable mode. Further, we note, from the asymptotic expressions, that the cell contracts as the porous paramter (i.e., as the permeability) decreases and convection sets in much earlier. An important thing to be noted in this context is that the differing nature of the wavenumber in the non-rotating and rotating systems. In the non rotating case I, it assumes the constant value unity whereas in the latter case the wavenumber is a function of P_L and $\mathcal{J}$. We know from the definition that, $\mathcal{J}_1^2$ is inversely proportional to the square of the viscosity; hence from the asymptotic expresstion for λ_0^* it follows that the actual temperature difference $(T_H - T_C)$ decreases with increasing viscosity. These destabilizing effects of viscosity and $1/P_L$ play an important role and we shall discuss these later with reference to finite amplitude motions.

Overstability

The striking similarity that exists on several occasions between the results pertaining to a fluid and a porous medium makes one to anticipate overstable motions in the present study. Therefore, in this section, we discuss infinitesimal overstable motions.

The imposed external constraint, such as rotation, suggests that p may be complex for $\mathcal{J}^2 > 0$, while it is real for $\mathcal{J}^2 = 0$. Therefore the cubic equation (3.7) has one real and two complex conjugate roots; hence we can write

$$(p_0 - p')\ (p_0 - p_r + ip_i)\ (p_0 - p_r - ip_i) = 0 \qquad \ldots(3.10)$$

or

$$P_0^3 - (p' + 2p_r)\ p^2 + (2p_r\, p' + p_i^2 + p_r^2)\ p_0 - p'\,(p_i^2 + p_r^2) = 0 \qquad \ldots(3.11)$$

where p', p_i and p_r all real. The condition for marginal stability requires that $p_r = 0$ and therefore, from (3.11) we have

$$P_0^3 - P^1\ P_0^2 + P_i^2 P_0 - P^1\ P_i^2 = 0. \qquad \ldots(3.12)$$

That is, for marginal stability, the product of the coefficients of p_0^2 and p_0 must be equal to the coefficient of p_0^0.

Applying this conditions to (3.11)

$$\lambda_0^* = \frac{2/P_L[(\alpha^2 + n^2)\,(\sigma/P_L + \pi^2(\alpha^2 + n^2))^2 + \mathcal{J}^2 n^2 \sigma^2]}{\alpha^2(\sigma/P_L + \pi^2(\alpha^2 + n^2))} \qquad \ldots(3.13)$$

which attains a minimum when

$$\partial\lambda_0^*/\partial\alpha^2 = 0. \qquad \ldots(3.14)$$

In the remainder of this analysis, our attention is restricted to the case $n=1$.

In (3.12), the coefficient of p_0 is a positive real quantity when p_0 is imaginary and hence from (3.11) we obtain the condition

$$p_i^2 = \frac{\sigma}{P_L}\left(\frac{\sigma}{P_L} + 2\pi^2\,(\alpha^2 + 1)\right) + \frac{\sigma}{(\alpha^2 + 1)}\,(\mathcal{J}^2\sigma - \alpha^2\lambda_0^*) > 0.$$

Substitution of (3.13) into the above equation gives the inequality

$$p_i^2 = -\frac{\sigma^2}{P_L^2} + \frac{y^2\sigma^2}{\alpha^2\pi^2}\left[1 - \frac{2\sigma}{\sigma + \pi^2 P_L\,(\alpha^2 + 1)}\right] \geq 0. \qquad \ldots(3.15)$$

Therefore, a necessary and sufficient condition for the occurrence of overstable motion is

$$\mathcal{J}^2 \geq \frac{\alpha^2 + 1}{P_L^2}\left[\frac{\sigma + \pi^2\,(\alpha^2 + 1)\,P_L}{-\sigma + \pi^2\,(\alpha^2 + 1)\,P_L}\right] \qquad \ldots(3.16)$$

and which in turn imposes a condition on σ viz.,

$$\sigma/P_L < \pi^2\,(\alpha^2 + 1)$$

or

$$\sigma < \pi^2 P_L\,(\alpha^2 + 1). \qquad \ldots(3.17)$$

In the case of rotating convective flow through a porous medium, overstable motions are possible only for small values of $\sigma (\sim 10^{-5})$ since $P_L \leq 10^{-4}$. But in most of the practical problems, σ is not so small and hence the condition (3.17) will be violated. Thus, the most important conclusion we can draw from this is, that overstable motions cannot occur unless the Prandtl number is extremely small ($\approx 10^{-5}$). This marks a definite point of departure from the results of Veronis[10], where time-dependent (overstable) motions occur to offset the stabilizing effect of rotation.

The foregoing discussion on the stability problem has provided information concerning the onset of steady convective instability and overstability and leaves the amplitude of the motion undetermined for a given value of λ^*. When the values of the relevant parameters are well above the critical conditions, linear theory cannot be called upon to explain the horizontal scale of motion, it simply predicts that unstable modes grow exponentially in time and provides no mechanism for the flow to reach a steady state. However, as the amplitude of motion increases, interactions of finite amplitude modes with each other become important and these effects are to be included in the nonlinear treatment of the problem, to get accurate results. Only a finite amplitude study can throw light on some of these unknown features like amplitude of the motion, energetics of the fluid, the preferred cell pattern for a given set of external parameters etc. We shall take up this study in the next section.

4. General Finite Amplitude Steady Convection

The complete set of required basic equations from (2.1) to (2.4) with $\partial/\partial t = 0$, can be written corresponding to different powers of ϵ, with the use of (2.6) in the following way:

$$\mathcal{L} W_0 = -\left[\frac{1}{P_L^2}\nabla^4 + \mathcal{J}^2\nabla^2\frac{\partial^2}{\partial z^2} + \frac{1}{P_L}\lambda_0^*\nabla_1^2\right] W_0 = 0$$

$$\mathcal{L} W_1 = \frac{1}{P_L}\lambda_1^*\nabla_1^2 W_0 - \mathcal{J}\nabla^2\frac{\partial z_{00}}{\partial z} - \frac{1}{P_L}\nabla_1^2 h_{00} - \frac{1}{P_L}\nabla^2 L_{00}$$

$$\mathcal{L} W_2 = \frac{1}{P_L}\lambda_2^*\nabla_1^2 W_1 + \frac{1}{P_L}\lambda_1^*\nabla_1^2 W_1 - \frac{1}{P_L}\nabla^2(L_{01} + L_{10})$$
$$- \mathcal{J}\nabla^2\frac{\partial}{\partial z}(Z_{01} + Z_{10}) - \frac{1}{P_L}\nabla_1^2(h_{01} + h_{10})$$
$$+ \frac{\sigma}{P_L}[W_0 T_0\}_m - \overline{W_0 T_0}]\nabla_1^2 W_0 \qquad \ldots(4.1)$$

$$-\nabla^2 T_0 = \sigma\lambda_0^* W_0$$
$$-\nabla^2 T_1 = \sigma\lambda_0^* W_1 + \sigma\lambda_1^* W_0 - \sigma h_{00}$$
$$-\nabla^2 T_2 = \sigma\lambda_0^* W_2 + \sigma\lambda_1^* W_1 + \sigma\lambda_2^* W_0 + \sigma^2[W_0 T_0\}_m - \overline{W_0 T_0}] W_0$$
$$- \sigma(h_{01} + h_{10}) \qquad \ldots(4.2)$$

$$\frac{1}{P_L}\zeta_0 = \mathcal{J}\frac{\partial W_0}{\partial z}$$

$$\frac{1}{P_L}\zeta_1 = \mathcal{J}\frac{\partial W_1}{\partial z} - Z_{00}$$

$$\frac{1}{P_L}\overset{*}{\zeta}_2 = \mathcal{J}\frac{\partial W_2}{\partial z} - (Z_{01} + Z_{10}) \qquad \ldots(4.3)$$

$$\frac{\partial u_i}{\partial x_i} + \frac{\partial v_i}{\partial y_i} + \frac{\partial W_i}{\partial z_i} = 0, \ (i = 0, 1, 2) \qquad \ldots(4.4)$$

where $\mathcal{L}$ is a constant linear operator.

We can develop higher-order solutions from the first-order solutions by the method of iteration. Here the subscript i corresponds to the order of the variables. The difficulties (appearance of resonant and secular terms) encountered in *I*, in determining the solution are also encountered in the present problem and the technique we employ in order to overcome these difficulties is exactly the same (i.e., the power integral technique) as used in *I*.

We now proceed to determine approximate finite-amplitude solution for two-dimensional rolls.

5. Finite Amplitude Solution for Rolls

Some qualitative features of the roll configuration is discussed in this section. The set of first-order solutions from (4.1) to (4.2) is given for the case of 2*D*-rolls with free surface. That is,

$$\left.\begin{aligned} W_0 &= 2\cos \pi\alpha x \sin n\pi z \\ T_0 &= 2\,\sigma\lambda_0^*/\pi^2\,(\alpha^2 + 1)\cos \pi\alpha x \sin n\pi z \\ V_0 &= \frac{2}{\alpha}\,\mathcal{J}P_L \sin \pi\alpha x \cos n\pi z \\ U_0 &= -\frac{2}{\alpha}\sin \pi\alpha x \cos n\pi z \end{aligned}\right\} \qquad \ldots(5.1)$$

where the values of the horizontal wavenumber α and λ_0^* are given by (3.8) and (3.10) for a particular value of $\mathcal{J}_1$.

The second order solution W_1 given by (4.1) involves the quantities Z_{00}, L_{00} and h_{00} in the inhomogeneous part and are of the form,

$$Z_{00} = \frac{\partial}{\partial z}(\vec{q}_0, \nabla v_0) - \frac{\partial}{\partial y}(\vec{q}_0, \nabla u_0) = -4\pi^2\mathcal{J}P_L \cos 2\pi\alpha x$$

$$L_{00} = \frac{\partial}{\partial z}\left[\frac{\partial}{\partial x}(\vec{q}_0 \cdot \nabla u_0) + \frac{\partial}{\partial y}(\vec{q}_0 \cdot \nabla v_0)\right] - \nabla_1^2\,\vec{q}_0 \cdot \nabla W_0 = 0$$

$$h_{00} = \vec{q}_0 \cdot \nabla T_0 - \frac{\partial}{\partial z}\overline{(W_0 T_0)}. \qquad \ldots(5.2)$$

Finally we have

$$W_1 = T_1 = U_1 = 0$$

$$V_1 = \frac{2}{\alpha} \mathfrak{L} P_L^2 \pi \sin 2\pi\alpha x$$

$$\lambda_2^* = \frac{\sigma^2 \lambda_0^*}{2\pi^2 (\alpha^2 + 1)} - \frac{2\pi^4 \mathfrak{J}^2 P_L^3 (\alpha^2 + 1)}{\alpha^2} \qquad \ldots(5.3)$$

Since $\lambda_1^* - 0$, (5.3) provides the first finite amplitude result.

It is not not necessary that an infinitesimal amplitude disturbance be the first to grow. We know that instability is often initiated by the nonlinear effects of small but finite disturbances. Therefore, this finite amplitude analysis which is based on the linear stability analysis predicts when the linear theory is meaningful. We know that subcritical solutions are possible only when λ_2^* is negative (Lortz[4]) and this is also clear from the expression for the convective heat transport. When λ_2^* is negative. λ^* given by (2.6) will be always smaller than λ_0^*, since ϵ^2 is positive. Hence, a steady solution with small but finite amplitude is unstable. If $\lambda_2^* > 0$, a real amplitude ϵ would be impossible for $\lambda^* < \lambda_0^*$. In other words, the linear stability theory would predict the lowest Rayleigh number at which the fluid becomes unstable.

6. Convective Heat Transport

Nusselt number Nu, is defined as the ratio of the actual heat transport rate to the rate at which heat would be transported by conduction for the given temperature difference between the hot and cold layers when convection is absent.

$$Nu = \frac{H}{\kappa \beta_m} = 1 + \frac{\sigma}{\lambda^*} \{WT\}_m \qquad \ldots(6.1)$$

where W and T are dimensionless and H is the vertical heat flux. In order to obtain the expression for the convective heat transport in known quantities, it is convenient to express $[WT]_m$ as a series in ϵ by expanding W ant T as in (2.6).
Hence,

$$\begin{aligned} \{WT\}_m = \epsilon^2 [\{W_0 T_0\}_m &+ \epsilon \{(W_0 T_1 + W_1 T_0)\}_m \\ &+ \epsilon^2 \{W_0 T_2 + W_1 T_1 + W_2 T_0\}_m \\ &+ \epsilon^3 \{W_0 T_3 + W_1 T_2 + W_2 T_1 + W_3 T_0\}_m \\ &+ \epsilon^4 \{W_0 T_4 + W_1 T_3 + W_2 T_2 + W_3 T_1 + W_4 T_0\}_m + \ldots] \end{aligned} \qquad \ldots(6.2)$$

Hence, to the third approximation, we obtain

$$\epsilon^2 = (\lambda^* - \lambda_0^*)/\lambda_2^* \qquad \ldots(6.3)$$

and

$$\frac{\sigma}{\lambda^*} \{WT\}_m = \frac{\sigma}{\lambda_2^*} \left(1 - \frac{\lambda_0^*}{\lambda^*}\right) \{W_0 T_0\}_m$$

$$= \frac{\sigma^2 \lambda_0^*}{\pi^2 (\alpha^2 + 1) \lambda_2^*} [1 - \lambda_0^*/\lambda^*] \qquad \ldots(6.4)$$

which gives a linear relation between the convection heat transport and λ^* and shows that the heat transport varies inversely as λ_2^*. Further, the slope of the heat transport curve is given by

$$\left.\frac{dNu}{d\lambda^*}\right|_{\lambda^*=\lambda_0^*} = \frac{\sigma^2}{\pi^2(\alpha^2 + 1)\lambda_2^*} \qquad ...(6.5)$$

which is a function of the rotational constraint, P_L and σ. Proceeding in the same manner, we finally compute the heat transport for the λ_4^*-approximation in the following way :

$$\frac{H}{\kappa\beta_m} = 1 + \sigma\frac{\epsilon^2}{\lambda^*}\left\{\frac{\sigma\lambda_0^*}{\pi^2(\alpha^2 + 1)} + \frac{E}{2}\epsilon^2\right\} \qquad ...(6.6)$$

Table II contains the computed values of *Nu* for a set of physical paramters.

TABLE I

λ_4^* for rolls

$\mathcal{J}_1^2$	$P_L^{-1} = 10^3$		$P_L^{-1} = 10^4$		$P_L^{-1} = 10^5$	
	λ_4^* (mercury)	λ_4^* (air)	λ_4^* (mercury)	λ_4^* (air)	λ_4^* (mercury)	λ_4^* (air)
0.1	0.2886×10^{-5}	0.1645×10	0.2885×10^{-4}	0.1645×10^{2}	0.2885×10^{-3}	0.1645×10^{3}
0.5	0.2887×10^{-5}	0.1645×10	0.2885×10^{-4}	0.1645×10^{2}	0.2885×10^{-3}	0.1645×10^{3}
1.0	0.2888×10^{-5}	0.1645×10	0.2885×10^{-4}	0.1645×10^{2}	0.2885×10^{-3}	0.1645×10^{3}
5.0	0.2896×10^{-5}	0.1645×10	0.2885×10^{-4}	0.1645×10^{2}	0.2885×10^{-3}	0.1645×10^{3}
10	0.2907×10^{-5}	0.1645×10	0.2885×10^{-4}	0.1645×10^{2}	0.2885×10^{-3}	0.1645×10^{3}
10^2	0.3099×10^{-5}	0.1648×10	0.2886×10^{-4}	0.1645×10^{2}	0.2885×10^{-3}	0.1645×10^{3}
10^3	0.4942×10^{-5}	0.1668×10	0.2886×10^{-4}	0.1645×10^{2}	0.2885×10^{-3}	0.1645×10^{3}
10^4	0.1897×10^{-4}	0.1842×10	0.2890×10^{-4}	0.1648×10^{2}	0.2886×10^{-3}	0.1645×10^{3}
10^5	0.7850×10^{-4}	0.2660×10	0.2931×10^{-4}	0.1668×10^{2}	0.2886×10^{-3}	0.1645×10^{3}
10^6	0.2586×10^{-3}	0.4393×10	0.3268×10^{-4}	0.1838×10^{2}	0.2890×10^{-3}	0.1648×10^{3}
10^7	-0.2610×10^{-1}	0.6231×10	0.4829×10^{-4}	0.2646×10^{2}	0.2925×10^{-3}	0.1648×10^{3}
10^8	-0.9751×10^{0}	0.6618×10	0.8137×10^{-4}	0.4348×10^{2}	0.3225×10^{-3}	0.1833×10^{3}

TABLE II

Value of ϵ^2 and Nu for rolls (λ_4^*-approximation)

$(\lambda_0^*/\lambda^*)^{-1}$	ϵ^2	*Nu*	ϵ^2	*Nu*
	$P_L^{-1} = 10^3$, $\mathcal{J}_1^2 = 0.1$, $\sigma = 0.0.25$		$P_L^{-1} = 10^3$, $\mathcal{J}_1^2 = 10^2$, $\sigma = 0.025$	

(*Continued on p.* 454)

TABLE II (*contd.*)

$(\lambda_0^*/\lambda^*)^{-1}$	ϵ^2	*Nu*	ϵ^2	*Nu*
1	0.0000	1.0000	0.0000	1.0000
2	0.5110×10^5	0.1809×10	0.5084×10^5	0.1799×10
3	0.8941×10^5	0.1943×10	0.8846×10^5	0.1923×10
4	0.1214×10^6	0.1961×10	0.1197×10^6	0.1934×10
5	0.1494×10^6	0.1946×10	0.1479×10^6	0.1916×10
	$P_L^{-1} = 10^3$, $\mathcal{G}_1^2 = 10^3$, $\sigma = 0.0.25$		$P_L^{-1} = 10^3$, $\mathcal{G}_1^2 = 10^4$, $\sigma = 0.025$	
1	0.0000	1.0000	0.0000	1.0000
2	0.4897×10^5	0.1724×10	0.4474×10^5	0.1439×10
3	0.8207×10^5	0.1783×10	0.6713×10^5	0.1364×10
4	0.1088×10^6	0.1759×10	0.8442×10^5	0.1288×10
5	0.1319×10^6	0.1719×10	0.9902×10^6	0.1227×10
	$P_L^{-1} = 10^3$, $\mathcal{G}_1^2 = 10^5$, $\sigma = 0.0.25$		$P_L^{-1} = 10^3$, $\mathcal{G}_1^2 = 0.1$, $\sigma = 0.687$	
1	0.1452×10^5	0.1172×10	0.0000	1.0000
2	0.5576×10^5	0.1097×10	0.6767×10^2	0.180910
3	0.7547×10^5	0.9868	0.1184×10^3	0.1943×10
4	0.9065×10^6	0.9183	0.1607×10^3	0.1061×10
5	0.1034×10^6	0.8716	0.1979×10^3	0.1946×10
	$P_L^{-1} = 10^3$, $\mathcal{G}_1^2 = 10^2$, $\sigma = 0.687$		$P_L^{-1} = 10^3$, $\mathcal{G}_1^2 = 10^3$, $\sigma = 0.687$	
1	0.0000	1.0000	0.0000	1.0000
2	0.6782×10^2	0.1808×10	0.6913×10^2	0.1807×10
3	0.1186×10^3	0.1943×10	0.1208×10^3	0.1940×10
4	0.1611×10^3	0.1960×10	0.1640×10^3	0.1957×10
5	0.1983×10^3	0.1946×10	0.2018×10^3	0.1942×10
	$P_L^{-1} = 10^3$, $\mathcal{G}_1^2 = 10^4$, $\sigma = 0.687$		$P_L^{-1} = 10^3$, $\mathcal{G}_1^2 = 10^5$, $\sigma = 0.687$	
1	0.0000	1.0000	0.0000	1.0000
2	0.7990×10^2	0.1794×10	0.1327×10^3	0.1740×10
3	0.1387×10^3	0.1918×10	0.2249×10^3	0.1835×10

TABLE II (*contd.*)

$(\lambda_0^*/\lambda^*)^{-1}$	ϵ^2	Nu	ϵ^2	Nu
4	0.1876×10^{3}	0.1931×10	0.3000×10^{3}	0.1835×10
5	0.2303×10^{3}	0.1914×10	0.3651×10^{3}	0.1812×10
	$P_L^{-1}=10^4$, $\mathcal{J}_1^2=0.1$, $\sigma=0.025$		$P_L^{-1}=10^4$, $\mathcal{J}_1^2=10^5$, $\sigma=0.025$	
1	0.0000	1.0000	0.0000	1.0000
2	0.5110×10^{5}	0.1809×10	0.5221×10^{5}	0.1807×10
3	0.8941×10^{5}	0.1943×10	0.9124×10^{5}	0.1939×10
4	0.1214×10^{6}	0.1961×10	0.1238×10^{6}	0.1956×10
5	0.1494×10^{6}	0.1946×10	0.1523×10^{6}	0.1941×10
	$P_L^{-1}=10^4$, $\mathcal{J}_1^2=10^6$, $\sigma=0.025$		$P_L^{-1}=10^4$, $\mathcal{J}_1^2=10^7$, $\sigma=0.025$	
1	0.0000	1.0000	0.0000	1.0000
2	0.6036×10^{6}	0.1792×10	0.1002×10^{6}	0.1733×10
3	0.1047×10^{6}	0.1913×10	0.1695×10^{6}	0.1817×10
4	0.1414×10^{6}	0.1923×10	0.2255×10^{6}	0.1809×10
5	0.1735×10^{6}	0.1905×10	0.2740×10^{6}	0.1781×10
	$P_L^{-1}=10^4$, $\mathcal{J}_1^2=10^8$, $\sigma=0.025$		$P_L^{-1}=10^4$, $\mathcal{J}_1^2=0.1$, $\sigma=0.687$	
1	0.0000	1.0000	0.0000	1.0000
2	0.2309×10^{6}	0.1642×10	0.6767×10^{2}	0.1809×10
3	0.3749×10^{6}	0.1676×10	0.1184×10^{3}	0.1943×10
4	0.4893×10^{6}	0.1647×10	0.1607×10^{3}	0.1961×10
5	0.5872×10^{6}	0.1610×10	0.1979×10^{3}	0.1946×10
	$P_L^{-1}=10^5$, $\mathcal{J}_1^2=10^8$, $\sigma=0.025$		$P_L^{-1}=10^5$, $\mathcal{J}_1^2=0.1$, $\sigma=0.687$	
1	0.0.0000	1.0000	0.0000	1.0000
2	0.6033×10^{5}	0.1794×10	0.6767×10^{2}	0.180910
3	0.1047×10^{6}	0.1919×10	0.1184×10^{3}	0.1943×10
4	0.1417×10^{6}	0.1932×10	0.1607×10^{3}	0.1061×10
5	0.1739×10^{6}	0.1916×10	0.1979×10^{3}	0.1946×10

TABLE II (*contd.*)

$(\lambda_0^*/\lambda^*)^{-1}$	ϵ^2	*Nu*	ϵ^2	*Nu*
	$P_L^{-1} = 10^5$, $\mathcal{G}_1^2 = 10^5$, $\sigma = 0.687$		$P_L^{-1} = 10^5$, $\mathcal{G}_1^2 = 10^6$, $\sigma = 0.687$	
1	0.0000	1.0000	0.0000	1.0000
2	0.6769×10^2	0.1805×10	0.6782×10^2	0.1808×10
3	0.1184×10^3	0.1943×10	0.1186×10^3	0.1943×10
4	0.1608×10^3	0.1961×10	0.1611×10^3	0.1960×10
5	0.1979×10^3	0.1946×10	0.1983×10^3	0.1946×10
	$P_L^{-1} = 10^5$, $\mathcal{G}_1^2 = 10^7$, $\sigma = 0.687$		$P_L^{-1} = 10^5$, $\mathcal{G}_1^2 = 10^8$, $\sigma = 0.687$	
1	0.0000	1.0000	0.0000	1.0000
2	0.6913×10^2	0.1807×10	0.7990×10^3	0.1794×10
3	0.1208×10^3	0.1940×10	0.1387×10^3	0.1919×10
4	0.1640×10^3	0.1957×10	0.1876×10^3	0.1932×10
5	0.2018×10^3	0.1942×10	0.2303×10^3	0.1916×10
	$P_L^{-1} = 10^4$, $\mathcal{G}_1^2 = 10^5$, $\sigma = 0.687$		$P_L^{-1} = 10^4$, $\mathcal{G}_1^2 = 10^6$, $\sigma = 0.687$	
1	0.0000	1.0000	0.0000	1.0000
2	0.6913×10^2	0.1807×10	0.7990×10^2	0.1794×10
3	0.1208×10^3	0.1940×10	0.1387×10^3	0.1919×10
4	0.1640×10^3	0.1957×10	0.1876×10^3	0.1932×10
5	0.2018×10^3	0.1942×10	0.2303×10^6	0.1916×10
	$P_L^{-1} = 10^4$, $\mathcal{G}_1^2 = 10^7$, $\sigma = 0.687$		$P_L^{-1} = 10^4$, $\mathcal{G}_1^2 = 10^8$, $\sigma = 0.687$	
1	0.0000	1.000	0.0000	1.0000
2	0.1327×10^3	0.1741×10	0.3024×10^3	0.1662×10
3	0.2250×10^3	0.1838×10	0.4968×10^3	0.1725×10
4	0.3002×10^3	0.1839×10	0.6522×10^3	0.1714×10
5	0.3654×10^3	0.1817×10	0.7855×10^3	0.1687×10
	$P_L^{-1} = 10^5$, $\mathcal{G}_1^2 = 0.1$, $\sigma = 0.025$		$P_L^{-1} = 10^5$, $\mathcal{G}_1^2 = 10^5$, $\sigma = 0.025$	
1	0.0000	1.0000	0.0000	1.0000

TABLE II (*contd.*)

$(\lambda_0^*/\lambda^*)^{-1}$	ϵ^2	*Nu*	ϵ^2	*Nu*
2	0.5110×10^5	0.1809×10	0.5111×10^5	0.1809×10
3	0.8941×10^5	0.1943×10	0.8943×10^5	0.1943×10
4	0.1214×10^6	0.1961×10	0.1214×10^6	0.1961×10
5	0.1494×10^6	0.1946×10	0.1495×10^6	0.1946×10
	$P_L^{-1} = 10^5$, $\mathcal{J}_1^2 = 10^6$, $\sigma = 0.025$		$P_L^{-1} = 10^5$, $\mathcal{J}_1^2 = 10^7$, $\sigma = 0.025$	
1	0.0.0000	1.0000	0.0000	1.0000
2	0.5121×10^5	0.1808×10	0.5220×10^5	0.1807×10
3	0.8960×10^5	0.1943×10	0.9126×10^5	0.1940×10
4	0.1216×10^6	0.1960×10	0.1238×10^6	0.1957×10
5	0.1497×10^6	0.1946×10	0.1524×10^3	0.1942×10

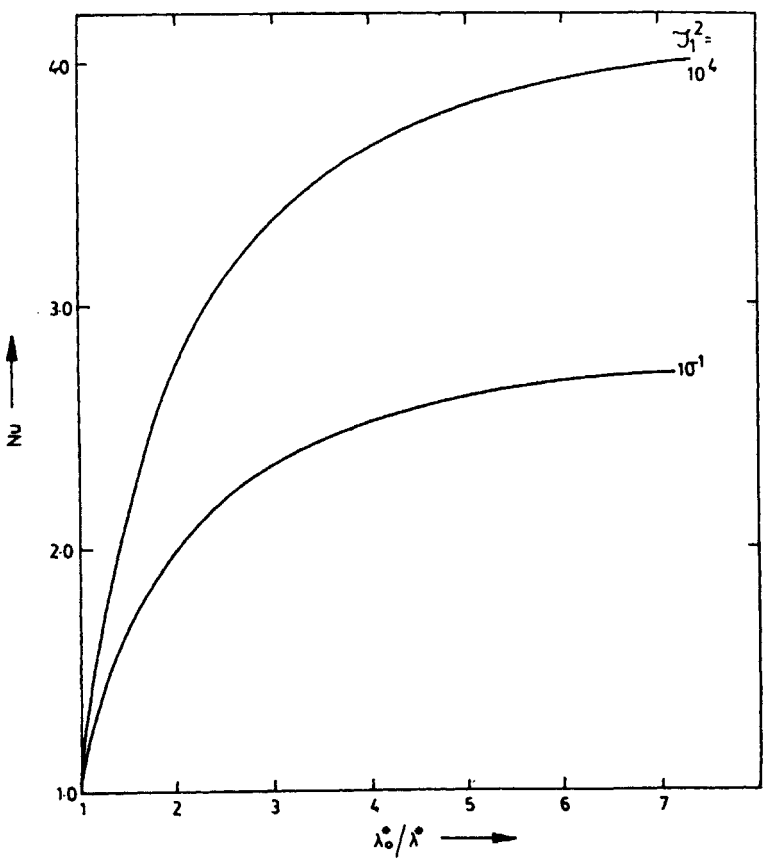

FIG. 3. *Nu* vs λ_0^*/λ^* for $\sigma = 0.025$ $P_L = 10^{-3}$ and various values of $\mathcal{J}_1^2$.

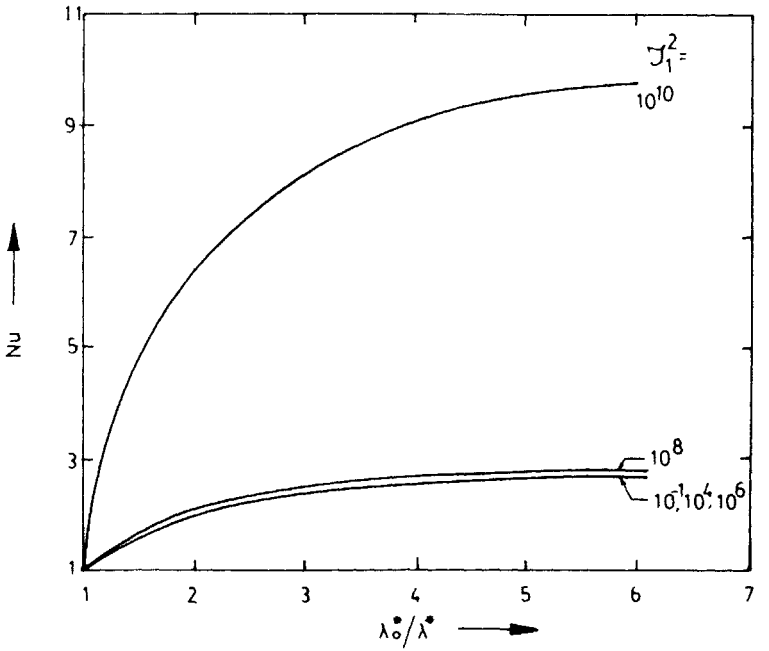

FIG. 4. *Nu* vs λ_0^*/λ^* for $\sigma = 0.687$, $P_L = 10^{-3}$ and various values of $\mathcal{J}_1^2$.

7. Discussion

Heat transport curves for rolls (second approximation) are presented in Figs. 3 to 9 for $\sigma = 0.025$, 0.687 and 6.87 corresponding to mercury, air and water respectively, and various values of $\mathcal{J}_1^2$ and P_L. A careful study of these reveals that the strong influences of σ and $\mathcal{J}_1^2$ on the heat transfer can be studied only for values of $P_L^{-1} \leq 10^3$ however, for values of $P_L^{-1} \geq 10^4$, neither σ nor $\mathcal{J}_1^2$ influence the heat transfer in the range $0.1 < \mathcal{J}_1^2$; which means that the heat transfer is not only independent of σ as in the non-rotating system I but also of the rotational constraint. However, for $\mathcal{J}_1^2 \geq 10^8$, the physical parameters have considerable effect on *Nu*. The most interesting thing we note here is that for $P_L^{-1} \geq 10^5$, the expression $(\sigma\{WT\}_m/(\lambda^* - \lambda_0^*))$ assumes a constant value ($=2$), for any given values of σ, P_L^{-1} and $\mathcal{J}_1^2$, except when $\mathcal{J}_1^2 = 10^{16}$ (i.e., $\mathcal{J}_1 P_L = 10^3$) in which case the convective heat transfer takes the value 5.1987. Further, no subcritical instabillities occur for $P_L^{-1} \geq 10^4$ in the range $0.1 \leq \mathcal{J}_1^2 \leq 10^{10}$, since $\lambda_2^* > 0$ and $\epsilon^2 > 0$ always; but for $P_L^{-1} = 10^3$, only for $\sigma = 0.025$ and 0.1 subscritical motions arise at very large rotation rates. Our numerical computations show that subcritical motions are possible for very small values of Prandtl number when $\mathcal{J}_1^2 = 10^{10}$, $P_L^{-1} = 10^4$; and $\mathcal{J}_1^2 \geq 10^{16}$, $P_L^{-1} = 10^5$); which is consistent with the results of section 4. These values when compared to the viscous case of Veronis[12], shows that only for $P_L^{-1} = 10^3$ and $\sigma > 0.1$, the heat transfer will be more for all $\mathcal{J}_1^2 \geq 10^6$, whereas in other cases, it is less. Further more, the constant value (≈ 2), obtained in the present analysis for $P_L^{-1} \geq 10^5$ is exactly the same as the one obtained in the viscous case for $\sigma = 0.8$ and $\mathcal{J}_1^2 = 10^8$. Another interesting result is that for $P_L^{-1} = 10^4$, $\sigma = 0.025$ and $\mathcal{J}_1^2 = 10^{10}$, maximum heat

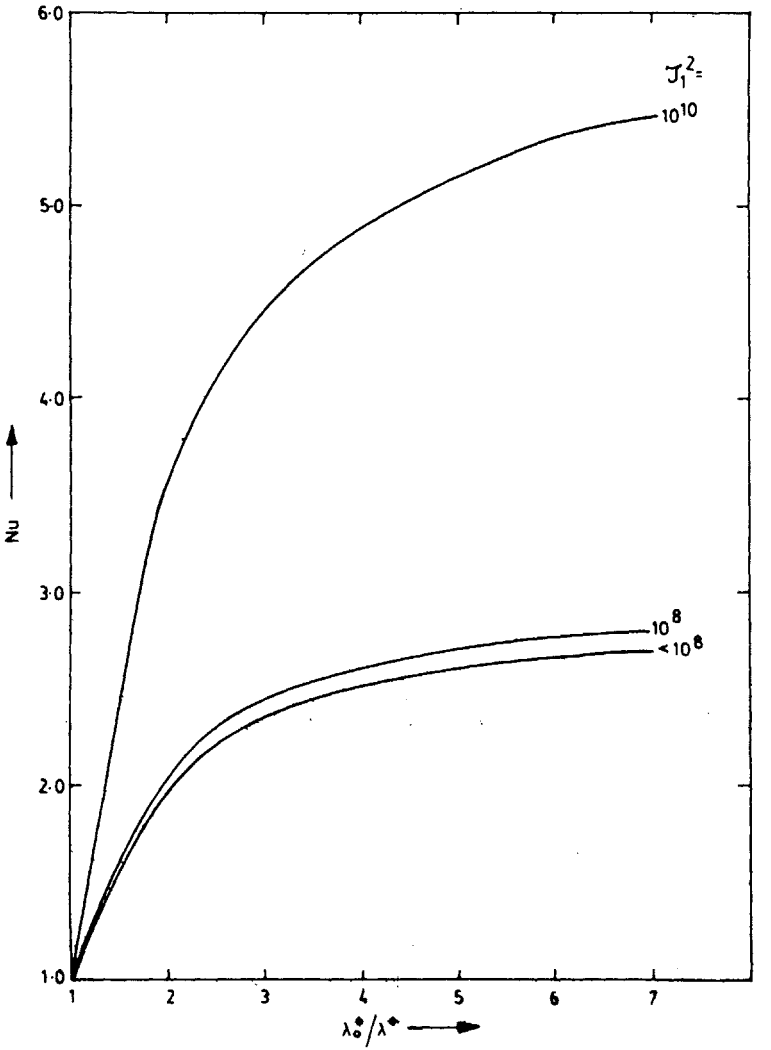

FIG. 5. *Nu* vs. λ_0^*/λ^* for $\sigma = 0.025$, $P_L = 10^{-4}$ and various values of $\mathcal{J}_1^2$

transport occurs for rolls. Mathematically it is justified that the effect of the non-linear momentum advection term is negligible, which is also physically meaningful.

Figure 9 illustrates the cumulative effect of the six modes, namely, $n = 1$, to 6 on the heat transfer for $\sigma = 6.87$, $P_L^{-1} = 10^4$ and $\mathcal{J}_1^2 = 10^8$ using the equation,

$$Nu = 1 \sum_{i=1}^{6} \sigma \{WT\}_m (1 - \lambda_{0i}/\lambda^*).$$

This procedure is justified by Catton[2], Rudraiah and Srimani[7], and Ruth[8]. Figure 9 reflects that there is a discrete change of slope of the heat flux curve at $\lambda^* = 3\lambda_0^*$ and $\lambda^* = 8\lambda_0^*$. In the figure, P_0, P_1 and P_2 represent the transition points. A Comparision of these results with those of Rudraiah and Srimani[7] shows ( ) the enhancement of the values of *Nu* in the absence of rotation and (ii) a markedly

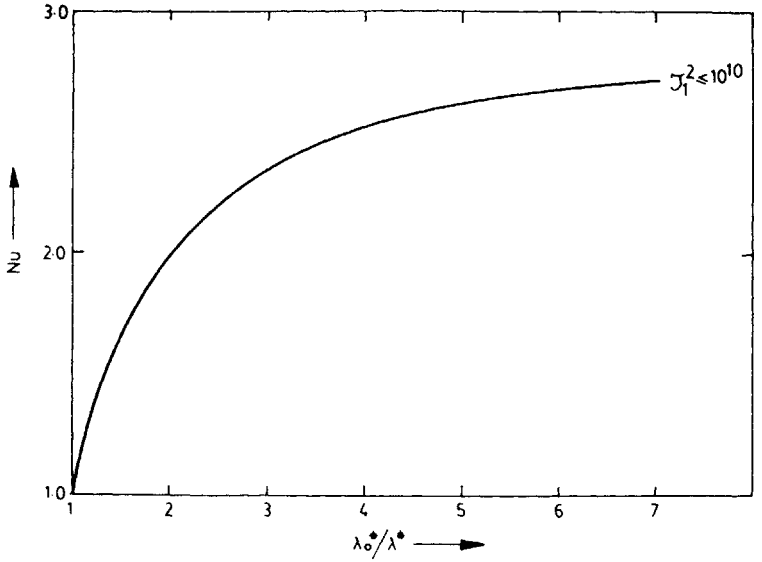

FIG. 6. *Nu* vs λ_0^*/λ^* or $\sigma = 0.687, 6.87$, $P_L = 10^{-4}$ and various values of $\mathcal{J}_1^2$.

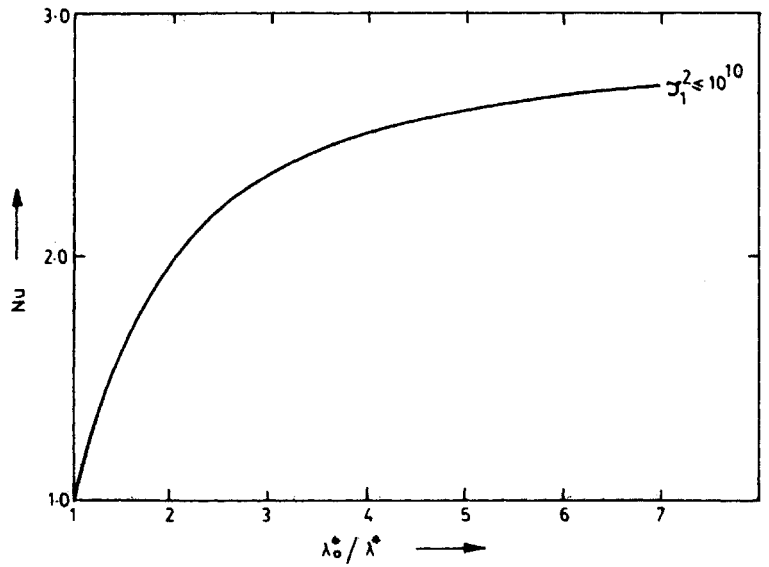

FIG. 7. *Nu* vs λ_0^*/λ^* for $\sigma = 0.025$, $P_L = 10^{-5}$ and various values of $\mathcal{J}_1^2$.

different behaviour of the rotating system from the non-rotating system. Upto the first transition point P_0, heat transfer is solely by conduction which is true for the first mode (the primary transition from conduction to convection), while the other transition points, if they actually occur will be between two convecting states. In each of the regions (for example, in P_1 P_2) all the six modes do not contribute (only $n = 1, 2$), and this can be explained as follows: In a horizontal layer of fluid, a number of discrete transitions occur before the flow becomes fully turbulent

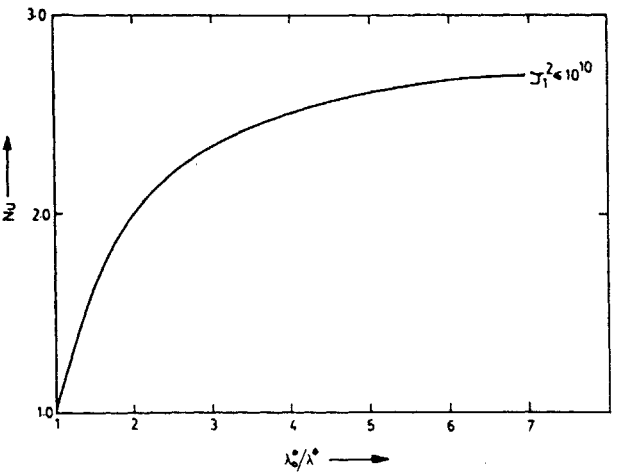

FIG. 8. *Nu* vs for $\sigma = 0.687, 6.87, 10$, $P_L = 10^{-5}$ and various values of $\mathcal{J}_1^2$.

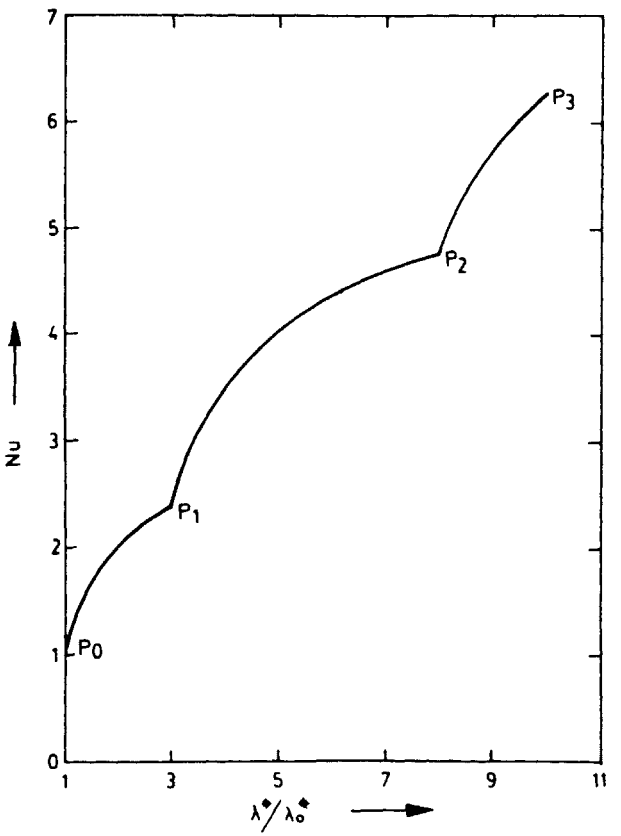

FIG. 9. Cumulative effect of the six modeg ($n=1,\ldots,6$) on *Nu* for $\sigma=6.87$ (water) $P_L = 10^{-4}$ and $\mathcal{J}^2 = 10^8$ in the case of rolls.

(Malkus[5]). The first is the well known transition at the critical Rayleigh number, from the conduction state to a steady two-dimensional convection. In this regime, a small non linear neighbourhood is reasonably well understood. As the value of λ^* is increased, the system becomes unstable to one kind of disturbance. As λ^* is increased still further, the fluid becomes unstable to more kinds of disturbances and at sufficiently large Rayleigh numbers, the flow is unstable to so many kinds of disturbances, each occurring with uncontrolled phase, that the flow may be called turbulent. Therefore, these transitions may be in plan-form, transition to time dependence etc., and the first well known transition is independent of the Prandtl number. Turning now to the analogous problem in a porous layer there is some evidence in the literature that the heat transfer in a porous layer suffers transitions similar to those by Malkus[5] in a fluid layer. For example, Palm at all[6] have detected transitions based on the experiments of Schneider[9], and Busse & Joseph[1] have detected a slope change in the heat transport curve. Therefore, we hope that this present result may be a good approximation to the experimental observations which are yet to be performed.

Acknowledgement

The authors wish to express their thanks to the UGC-DSA Centre, Department of Mathematics, Central College, Bangalore University, Bangalore for the encouragement.

References

1. F. H. Busse and D. D. Joseph, *J. Fluid Mech.* **54** (1972), 521.
2. I. Catton, *Phys. Fluids* **9** (1966), 2521.
3. S. Chandrasekhar, *Hydrodyanmic and Hydromagnetic Stability*, Oxford University Press, London, 1961.
4. D. Lortz, *J. Fluid Mech.* **23** (1965), 113.
5. W. V. R. Malkus, *Proc. R. Soc.***A 225** (1954), 196.
6. E. Palm, J. E. Weber and O. Kvernfold, *J. Fluid Mech.* **54** (1972), 153.
7. N. Rudraiah and P. K. Srimani, *Proc. R. Soc.* **A373** (1980), 199.
8. D. W. Ruth, *AIA 18th Aerospace Science Meeting* Jan. 14-16, Pasadena, California, 1980.
9. K. J. Sehneider, *11th Int. Cong. of Refrigeration,* Munich 1963.
10. P. K. Srimani, Ph.D thesis, Bangalore Univ., 1980.
11. J. S. Turner, Buoyancy effects in fluids. Cambridge University Press, Cambridge (1978).
12. G. Veronis, *J. fluid Mech.* **5** (1959), 401.